

Electronic Supplementary Information

Modular assembly of plasmonic core-satellites structures as highly brilliant SERS-encoded nanoparticles

Nicolas Pazos-Perez,^{a,*} Jamie M. Fitzgerald,^b Vincenzo Giannini,^{b,c} Luca Guerrini,^a Ramon A. Alvarez-Puebla^{a,d,*}

^a Departamento de Química Física e Inorgánica, and EMaS, Universitat Rovira i Virgili, Carrer de Marcel·lí Domingo s/n, 43007 Tarragona, Spain.

^b Department of Physics Condensed Matter Theory, Imperial College London, England.

^c Instituto de Estructura de la Materia (IEM-CSIC), Consejo Superior de Investigaciones Científicas, Serrano 121, 28006 Madrid, Spain

^d ICREA, Passeig Lluís Companys 23, 08010 Barcelona, Spain.

E-mail: nicolas.pazos@urv.cat; ramon.alvarez@urv.cat

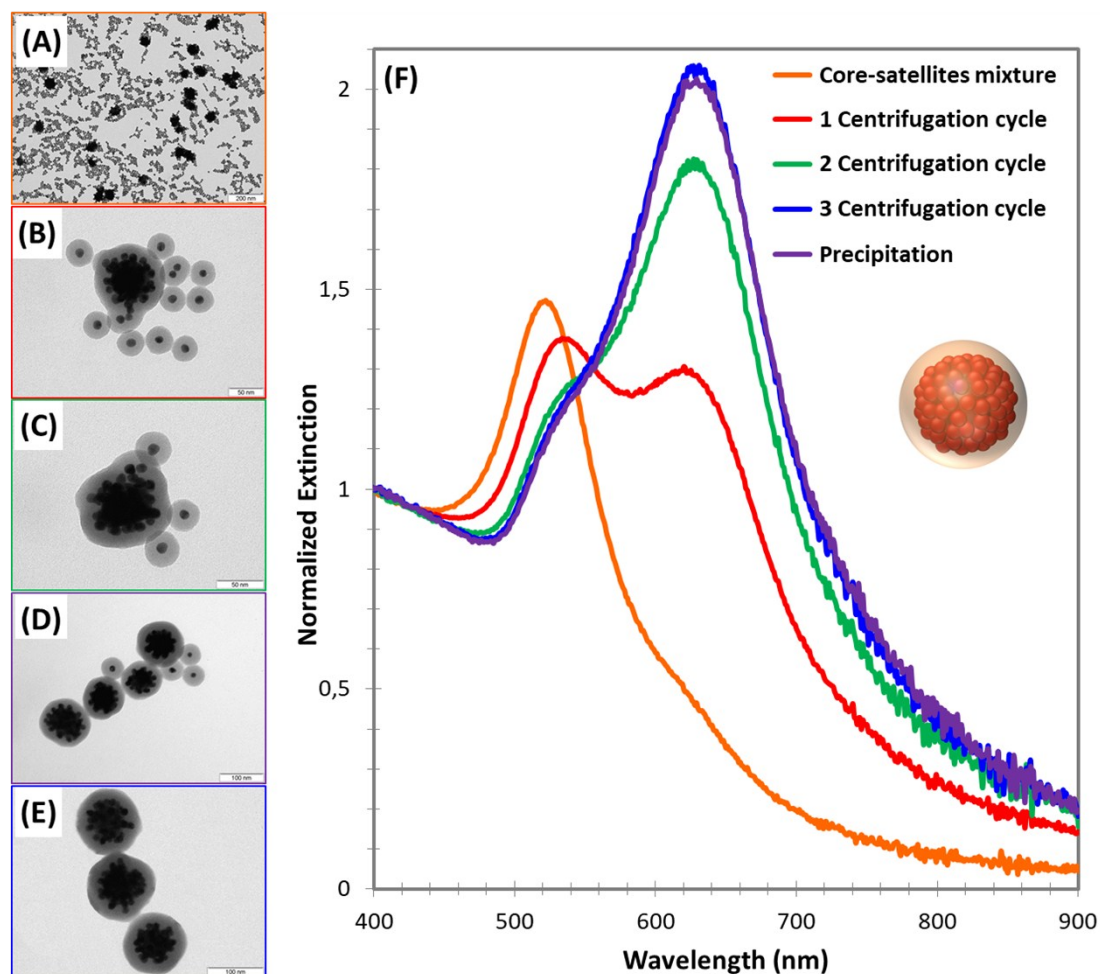


Figure S1. Representative TEM images illustrating the different steps of the core-satellites purification process post-silica encapsulation: (A) original particle mixtures (gold cores mixed with an excess of satellites), and upon (B, C, D) three centrifugation/washing cycles (1, 2, and 3, respectively), and, finally, a last step of separation via selective precipitation (E). The corresponding extinction spectra are plotted in (F).

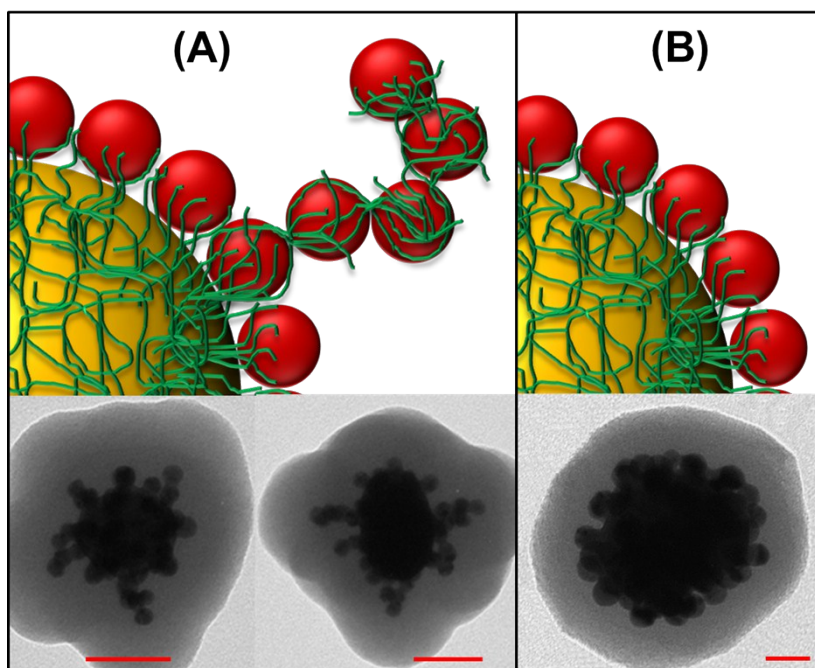


Figure S2. Representative TEM images of core-satellites assemblies, where core particles were subject of (A) 1 washing cycle upon addition of PEI (scale bars = 50 nm) or (B) 3 washing cycles (scale bar = 20 nm). The presence of unbound or loosely bound PEI is responsible for the formation of satellite-chain like structures protruding from the core particles.

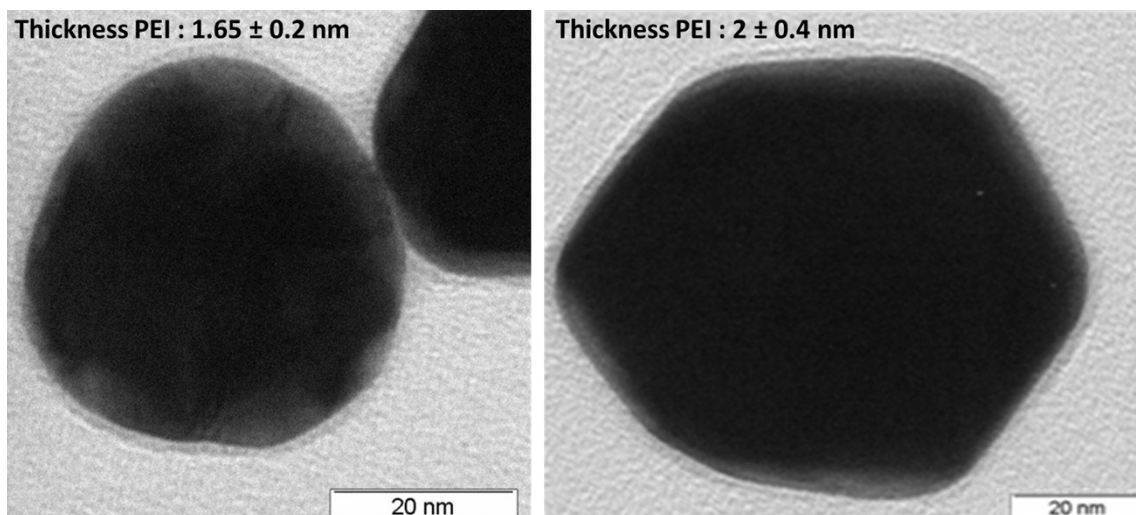


Figure S3. Representative TEM images of Au-cores functionalized with a mixed layer of MUA/MBA and then wrapped with PEI, prior to the addition of satellites.

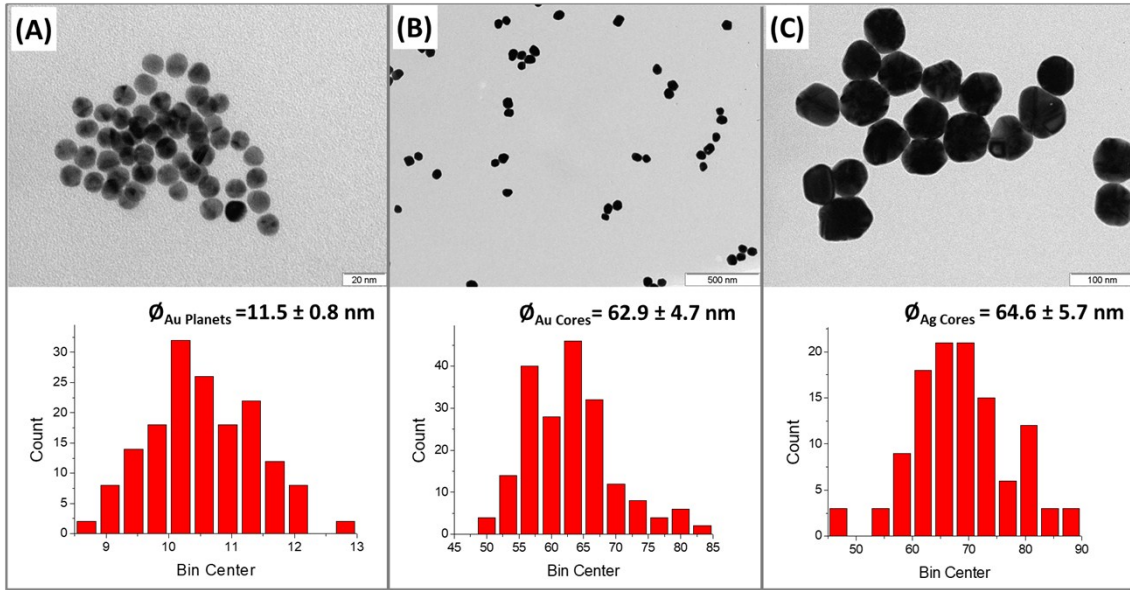


Figure S4. Representative TEM images of citrate-capped (A) Au-cores, (B) Au-satellites, and (C) Ag-cores; and their corresponding size-distribution histograms.

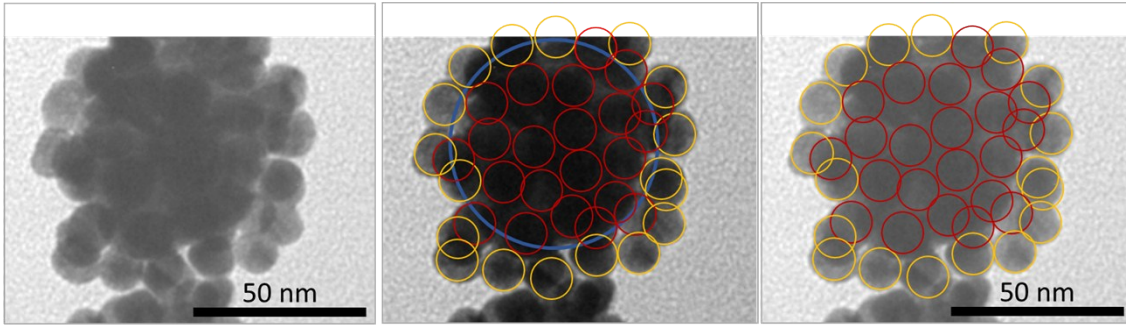


Figure S5. Satellite counting. 30 Au-core@satellite assemblies (63 nm and 12 nm diameters, respectively) were selected and individually analyzed as follows. A blue circle was drawn on the central core. Then, small circles were drawn on each satellite. Two groups of satellites were identified: (i) x satellites sitting on the half-hemisphere (red circles), and (ii) y satellites sitting at the external halo (yellow circles). Assuming that the number of satellites adsorbed on the opposite hemisphere is the same, the total number of satellites per core was estimated as:

$$\text{Total number of satellites per assembly} = 2x + y$$

This approach provides a rather conservative estimation of the satellite density since, as also shown in the representative TEM image reported in this figure, other satellites can be seen sitting behind the halo of yellow-encircled satellites (i.e., we underestimated the total number of satellites located at the halo of the other hemisphere).

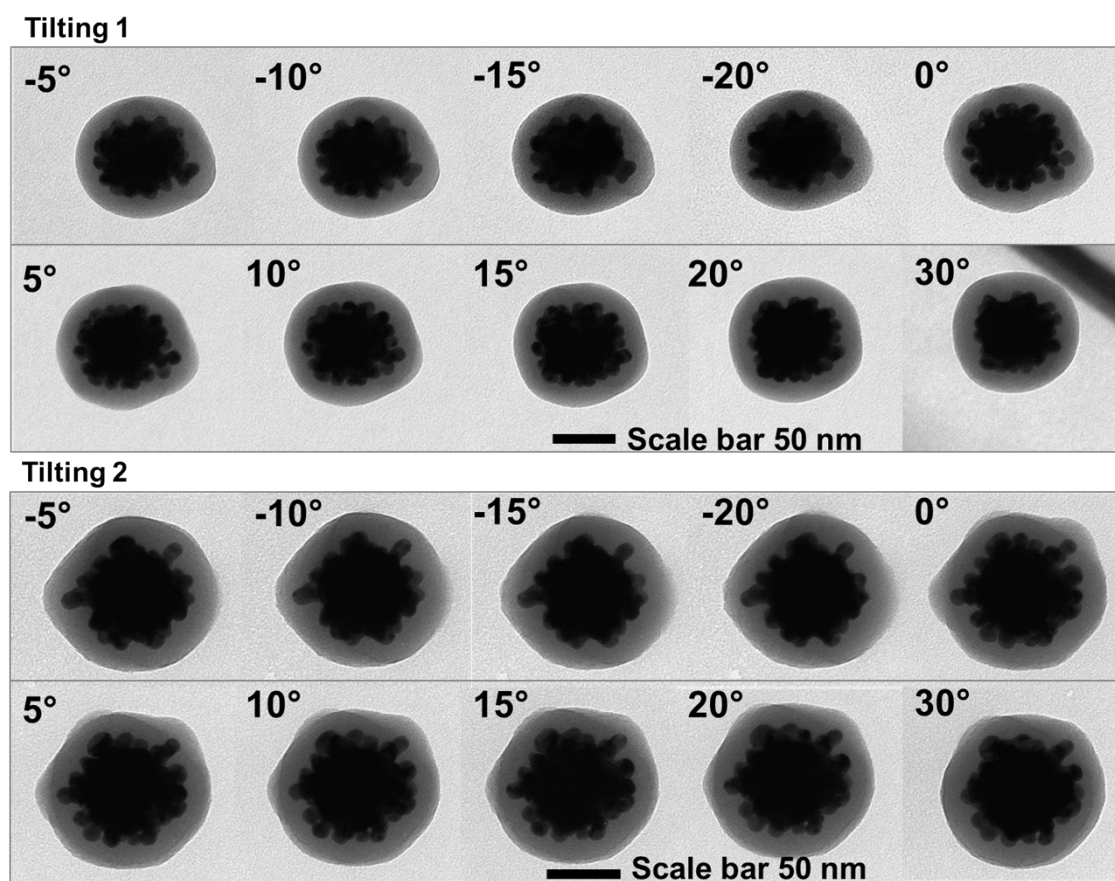


Figure S6. Series of TEM images of a representative core-satellite assembly tilted at different relative angles.

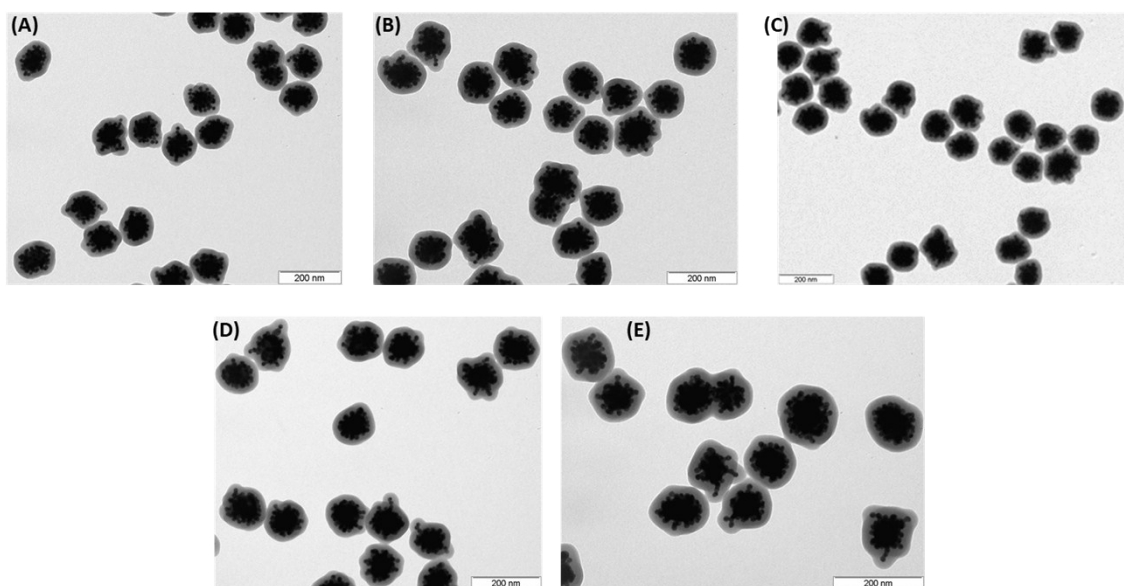


Figure S7. Figure S7. Representative TEM image of core-satellites comprising (A) Au-core@MUA/MBA and Sat@Cit; (B) Au-core@MUA/MBA and Sat@MUA/MBA; (C) Au-core@MUA/MBA and Sat@MUA/MBA; (D) Au-core@MUA/TP and Sat@MUA/TP and (E) Au-core@MUA/CV and Sat@MUA/CV. TP: Thiophenol; CV: Crystal Violet.

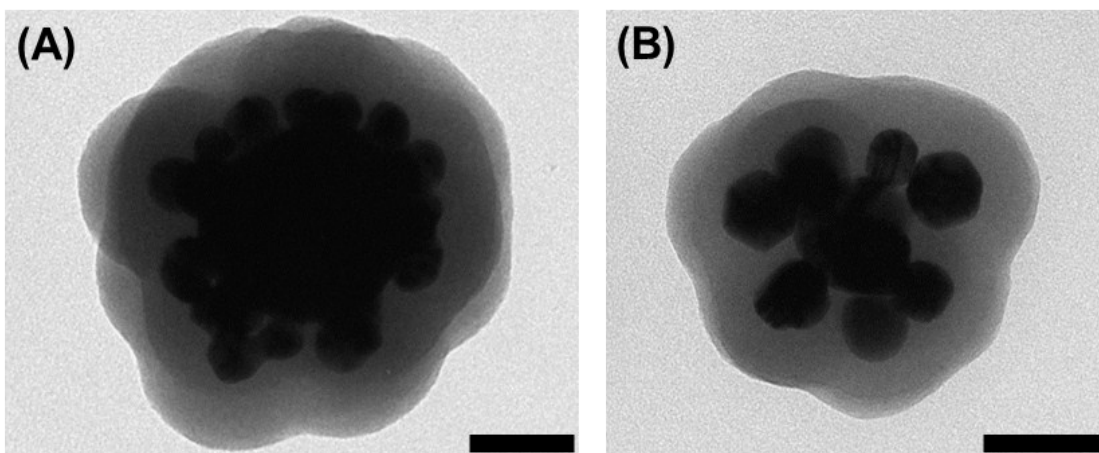


Figure S8. Representative TEM images illustrating core-satellites assemblies comprising (A) Au-core (ca. 95 nm diameter) and Au-satellites (ca. 25 nm diameter); and, (B) Ag-core (ca. 50 nm) and Au-satellites (ca. 30 nm diameter). Scale bar: 50 nm.